

Exciton localization effects and heterojunction band offset in (Ga,In)P-(Al,Ga,In)P multiple quantum wells

Martin D. Dawson and Geoffrey Duggan

Sharp Laboratories of Europe, Ltd., Edmund Halley Road, Oxford Science Park, Oxford OX4 4GA, United Kingdom

(Received 26 October 1992)

Disordered $\text{Ga}_{0.52}\text{In}_{0.48}\text{P}/(\text{Al}_{0.7}\text{Ga}_{0.3})_{0.52}\text{In}_{0.48}\text{P}$ bulk and quantum-well epilayers, lattice matched to GaAs substrates misoriented from (100), have been studied by low-temperature photoluminescence (PL) and photoluminescence excitation spectroscopy (PLE). The effects of excitonic weak localization are discussed by comparison between the PL and PLE data. Envelope-function fitting of the excitonic transitions observed in PLE has been used to determine a conduction-band discontinuity ΔE_c of $\sim 0.67\Delta E_g$, providing strong support for the value obtained by Liedenbaum *et al.* [Appl. Phys. Lett. **57**, 2699 (1990)].

I. INTRODUCTION

The (Al,Ga,In)P semiconductor system offers the widest direct energy gaps in the III-V alloys apart from nitrogen-containing compounds.¹ This fact, combined with the possibility of lattice matching to GaAs substrates, has made (Ga,In)P-(Al,Ga,In)P bulk and quantum-well heterostructures of great interest for optoelectronic applications in the visible-wavelength region below 700 nm.²

Determination of the fundamental physical parameters of the material, particularly the band-gap energies and heterojunction band offset, essential for optimal device design, has however been complicated by a number of factors. Both (Ga,In)P and (Al,Ga,In)P alloys are known to exhibit spontaneous long-range ordering on the group-III sublattice when deposited by the commonly used metal-organic chemical vapor deposition (MOCVD) growth technique. The lattice-matched ternary alloy $\text{Ga}_{0.52}\text{In}_{0.48}\text{P}$, for example, has been found to show CuPt-type ordering, taking the form of alternating GaP-InP layers along two of the four possible $\langle 111 \rangle$ directions, for growth in the range 650–700°C on (001) GaAs substrates.³ The ordering has the effect of lowering the band gap. This has been explained⁴ as arising from the doubling of the unit cell in the ordered alloy. The size of the Brillouin zone is thus halved and, as a consequence, the electronic states at the L point are zone folded back to the Γ point, repelling the like-symmetry conduction-band-edge Γ_{6c} states to lower energy. The degree of ordering has been found to be *strongly* dependent upon the exact growth conditions (temperature, growth rates, group V/group III gas-flow ratio, and substrate orientation), resulting in a variation in the reported band gap of up to ~ 135 meV (Ref. 5). In addition to possible influence by these growth-related effects, the majority of the attempts^{5–10} to determine the (Ga,In)P-(Al,Ga,In)P heterojunction band-offset ratio have (with the exception of Ref. 10) used the technique of low-temperature photoluminescence (PL), for which (i) the PL is assumed to be intrinsic, (ii) no account is taken of any “Stokes shift” between the PL and the dominant absorption edge, and (iii)

only the lowest-energy exciton ($e1\text{-hh}1$) transition is fitted. Given these considerations, it is perhaps not surprising that the band-offset ratio for this system is still in dispute, with reported values of the conduction-band discontinuity ΔE_c , ranging from $\sim 0.39\Delta E_g$ to $\sim 0.65\Delta E_g$ (Refs. 5–10). Here, we report determination of the band-offset ratio at the (Ga,In)P-(Al,Ga,In)P heterobarrier by low-temperature photoluminescence excitation spectroscopy (PLE), which avoids the complication of any Stokes shift and allows higher-lying exciton transitions to be measured in addition to the lowest-energy $e1\text{-hh}1$ transition. Quantum-well samples with well widths covering the range 14 to 120 Å were examined, grown under conditions chosen to minimize the effects of alloy ordering. A conduction-band discontinuity of $\Delta E_c \sim 0.67\Delta E_g$ is obtained by envelope-function fitting of the observed excitonic transitions and is compared to previously obtained values. Comparison between the PLE spectra and PL data has allowed the effects of exciton localization to be studied.

II. EXPERIMENT

The $\text{Ga}_{0.52}\text{In}_{0.48}\text{P}/(\text{Al}_{0.7}\text{Ga}_{0.3})_{0.52}\text{In}_{0.48}\text{P}$ samples, all nominally undoped, were grown by low-pressure MOCVD on semi-insulating GaAs substrates. Double crystal x-ray-diffraction rocking curve data, taken at room temperature, confirmed lattice matching of the epilayer to the substrate for all samples to within 0.02%. Each sample consisted of a 0.5- μm GaAs buffer, followed by a 1- μm (Al,Ga,In)P layer, then the active region of the structure, an (Al,Ga,In)P layer of thickness either 0.1 or 1 μm , and a final 0.02- μm GaAs protective cap. The active regions for the respective samples were (i) a 0.1- μm (Ga,In)P bulk layer, and (ii)-(vi) multiple quantum-well (MQW) samples, of between 1 and 50 periods, with nominal well widths 14, 30, 50, 75, and 120 Å, respectively. The accuracy of these well-width values is estimated to be better than 5% as determined from growth rates and subsequent transmission electron microscopy measurements on test samples grown in the same reactor under similar conditions.¹¹ All MQW samples had 100-Å (Al,Ga,In)P

barriers. A constant quaternary composition of $(\text{Al}_{0.7}\text{Ga}_{0.3})_{0.52}\text{In}_{0.48}\text{P}$ was used throughout, chosen to give the largest direct energy gap with lattice matching to GaAs.¹

Growth was performed simultaneously on half wafers of GaAs polished 2° and 10°, respectively, off (100) towards (110). All data reported here were taken on the 10° off samples, unless otherwise noted. The growth temperature was in excess of 700°C; the results obtained for the 2° and 10° off samples are consistent⁵ with data for other structures in the literature grown at ~760°C. It has been shown that spontaneous ordering in (Ga,In)P occurs due to surface rather than bulk thermodynamic effects during growth¹² and that its influence on the energy gap can be avoided either by using a growth temperature^{13,14} well in excess of 700°C, or by using substrates appropriately oriented to provide a large enough density of surface steps along the ordering diagonals of the unit cell.^{10,15,16} Transmission electron-diffraction studies¹⁷ on the 10° off bulk sample showed only very faint half period superstructure reflection spots appearing in long-exposure $[1\bar{1}0]$ zone-axis measurements and none evident in the $[110]$ zone-axis data. This is consistent¹⁶ with the alloy being predominantly random in nature, with residual ordering at an extremely low level. Additional evidence for effective elimination of ordering is given by PL data discussed below.

Measurements were performed at 5 K, with the samples mounted in a helium flow cryostat. PL and PLE data for the bulk sample were taken using a cw dye laser (Rhodamine 6G) excitation source, whereas all other PL and PLE data were obtained using a tungsten-halogen lamp/0.22-m monochromator combination. The detection system consisted of a 0.85-m double-grating spectrometer, cooled GaAs photomultiplier, and photon counting electronics. Overall spectral resolution for the PLE measurements was 5–10 Å.

III. RESULTS AND DISCUSSIONS

A. Bulk (Ga,In)P and (Al,Ga,In)P

PL and PLE spectra for the bulk $\text{Ga}_{0.52}\text{In}_{0.48}\text{P}$ sample are shown in Fig. 1. The PL peak is at 1.993 eV and has a full width at half maximum (FWHM) of 6.5 meV, which is comparable to the narrowest reported in the literature.^{5,10,14} The absence of ordering in the sample is supported by (i) the single-peaked nature of the PL and its narrow linewidth, (ii) the high-energy position of the PL peak (corresponding to previous reports for disordered material^{10,14}), (iii) the absence of saturation of PL intensity over three orders of magnitude in excitation fluence (as shown in Fig. 2), and (iv) observation of a shift (Fig. 2) to higher energy in the PL peak position of only 5 meV with increasing fluence over the same range (cf. Ref. 14). In addition, we have repeated the room-temperature polarized PL measurements of Mascarenhas *et al.*¹⁸ for our sample. Dye laser excitation light (625 nm) was linearly polarized along either $[001]$ (with a projection along the $[111]$ and $[\bar{1}\bar{1}\bar{1}]$ possible ordering directions in the crystal) or $[0\bar{1}\bar{1}]$ crystals axes (having no projection

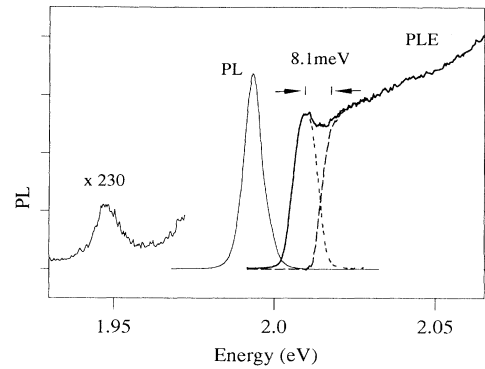


FIG. 1. 5-K PL and PLE spectra for bulk (Ga,In)P with expanded PL phonon replica inset, and decomposition of PLE spectrum into excitonic and continuum absorption components indicated.

along the possible ordering directions). No significant energy shift was observed (Fig. 3) between polarized PL detected either parallel or perpendicular to the excitation polarization in either case, providing further evidence¹⁸ of the disordered nature of the (Ga,In)P.

Returning to Fig. 1, the peak of the fundamental exciton in the PLE spectrum is observable at 2.01 eV, and just discernible to higher energy is the onset of the continuum absorption. By assuming a symmetrical form for the exciton peak and subtracting this graphically from the measured PLE data, the form of the continuum absorption edge can be obtained, as shown in the figure. From this, we can deduce the binding energy of the free exciton in bulk $\text{Ga}_{0.52}\text{In}_{0.48}\text{P}$ to be ~8.1 meV. This agrees well with a previous determination¹⁰ and is consistent with the value calculated using the standard hydrogenic model,¹⁰ with the effective masses being those used to provide fitting in the envelope-function calculations (see Table I), and a dielectric constant of $11.75\epsilon_0$ obtained by linear interpolation between the two binaries. Taking the exciton binding energy into account, the 5-K band gap or disordered, lattice-matched (Ga,In)P is determined to be 2.018 eV.

The PL is believed to be of an intrinsic nature in the sense of not being due to impurities in the sample, with

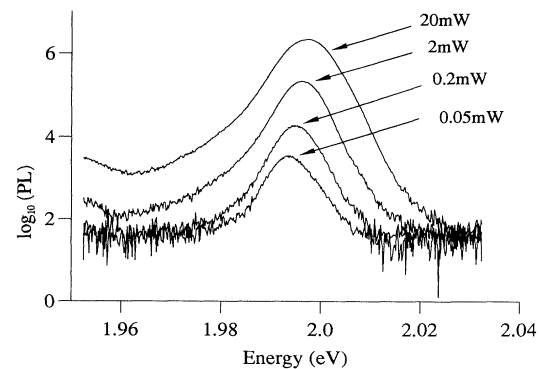


FIG. 2. Log plot of the fluence dependence of the 5-K PL from bulk (Ga,In)P. Spot size (FWHM intensity) ~ 100 μm .

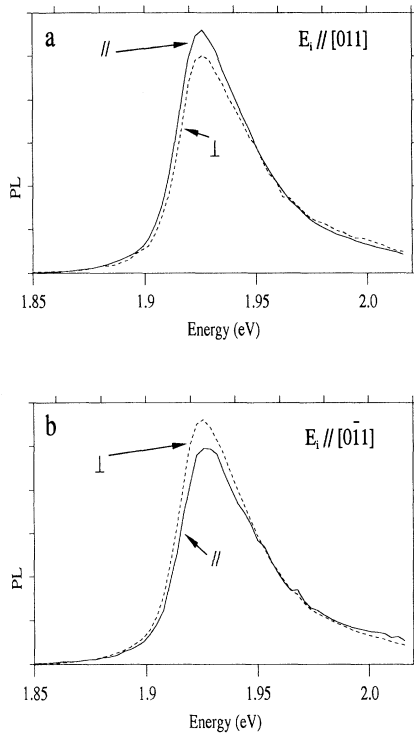


FIG. 3. Room-temperature polarized PL measurement with detection parallel and perpendicular to the excitation light for (a) excitation polarized parallel to [011] and (b) excitation polarized parallel to $[0\bar{1}1]$.

the observed Stokes shift of ~ 17 meV between the PL and exciton peaks being ascribed to localization of excitons at potential minima caused by “alloy disorder” compositional variations in the layer. Evidence supporting this assertion comes from the lack of alloy ordering and the following data. PL and PLE measurements were performed as a function of temperature in the range 5–120 K (Fig. 4). Up to ~ 60 K, the PLE peak stays essentially fixed in energy, whereas the PL line moves towards the PLE peak, i.e., to *higher energy*, by ~ 8 meV. Above 60 K, both PL and PLE shift monotonically to lower energy, reflecting the variation of the (Ga,In)P band gap with

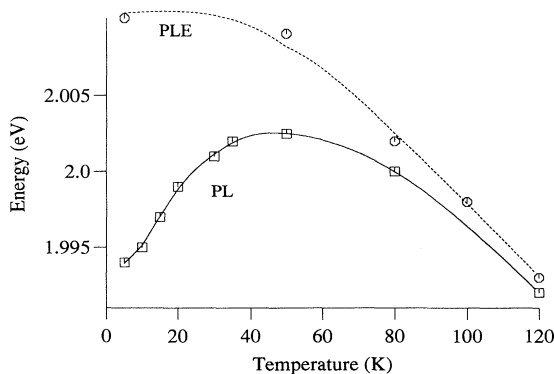


FIG. 4. Temperature dependence of the PL and PLE peaks for bulk (Ga,In)P.

temperature. The energy difference between the peaks decreases with temperature over this range, and they become almost coincident near 150 K. This behavior is not consistent with that expected for impurity-assisted recombination. The observations are interpreted in the following manner: microscopic fluctuations occur in the alloy composition of the (Ga,In)P and there will be regions where the local indium mole fraction is slightly higher than the lattice-matched composition, giving rise to a statistical distribution of local potential minima. At low temperatures, PL takes place from the lowest-energy states that can be occupied in the sample, and thus is dominated by excitons weakly bound at these potential minima. The Stokes shift at 5 K thus provides an indication of the maximum degree of local compositional fluctuation in the alloy—note in this context that an energy shift of 17 meV represents a change in local indium mole fraction of only ~ 1.4 at. % from the lattice-matched composition. As the temperature increases, the states to higher energy become occupied due to thermalization and the PL develops a high-energy tail and moves towards the PLE peak roughly as $\sim kT$, reflecting the larger density of states (and larger sample volume with this indium fraction) at the higher energy. The lack of saturation in the fluence-dependent PL measurement (Fig. 2) is not at odds with this interpretation: local potential minima states could constitute only a fraction of a percent of the free carrier density of states (thus not appearing strongly in the absorption) and still be present in large enough absolute density, or have a rapid enough recombination rate associated with them, to not be readily saturable.

A weak phonon-assisted satellite recombination peak (0.15% of the main PL peak intensity at 5 K) was observable ~ 47 meV below the main PL line—this is shown in the inset expanded PL curve of Fig. 1. Raman-scattering measurements^{19,20} on (Ga,In)P have shown a structured spectrum, with a strong LO mode at 380 cm^{-1} (47.2 meV) and a weaker mode at 360 cm^{-1} (44.6 meV), the origin and assignment of which are still under debate. Evidence²⁰ points to the latter mode being the InP-like LO mode and the former being the GaP-like LO mode. Due to the 6.5-meV linewidth of the PL, the close proximity of the two Raman modes, and the differing polarizabilities of the two binaries, we would not expect, however, to separately resolve GaP-like and InP-like phonon replicas. The polarization of the lattice associated with a weakly bound exciton is known to enhance coupling to LO photon modes,²¹ thus observation of phonon-assisted recombination provides additional evidence for excitonic localization. In support of this viewpoint, the replica becomes weaker with increasing temperature, as we would expect for excitons thermalizing out of localized states, and becomes indistinguishable from the low-energy tail of the main PL line above 15 K. The phonon replica is responsible for the rising signal below 1.96 eV in the fluence-dependent PL measurements of Fig. 2.

PL and PLE were also performed (using the lamp excitation source) on the $(\text{Al}_{0.7}\text{Ga}_{0.3})_{0.52}\text{In}_{0.48}\text{P}$ in the sample—see Fig. 5. The exciton peak in PLE is at 2.439 eV, and the main PL peak (of FWHM 10.5 meV) is ob-

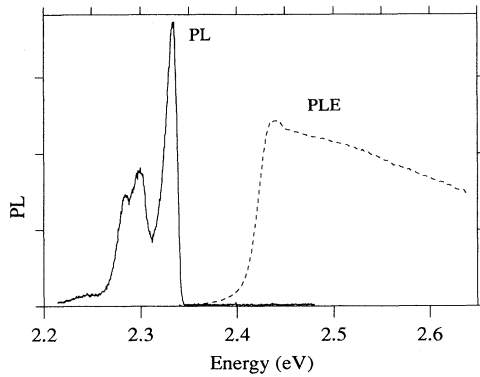


FIG. 5. 5-K PL and PLE spectra for (Al,Ga,In)P.

served at 2.334 eV. The same PLE spectrum was obtained for detection at all peaks in the distinctive PL line shape, indicating that the full PL line shape originates from the quaternary alloy. The PLE data has been corrected for the spectral response of the excitation source. We ascribe the decrease of the PLE signal above the band edge to the fact that the lattice-matched alloy $(\text{Al}_{0.7}\text{Ga}_{0.3})_{0.52}\text{In}_{0.48}\text{P}$ is at the crossover point between direct and indirect (k space) behavior.¹ The conduction band Γ and X states are therefore close to resonance and X states will become populated as the excitation light is tuned above the absorption edge, decreasing the signal detected at the PL line. The energy separation between the PL and PLE peaks does not decrease with increased temperature for the quaternary case. This, combined with its large magnitude (over 100 meV) leads us to ascribe the shift to an extrinsic process—possibly (neutral) donor-assisted recombination, as all samples are residually n type.¹¹

B. (Ga,In)P-(Al,Ga,In)P quantum wells

We now discuss the quantum-well samples. The 120-, 75-, and 50-Å well structures contained 50 periods, the 30-Å sample 5 periods, and the 14-Å sample a single period. Figure 6 summarizes the 5-K PL results obtained. We emphasize that this is a composite figure—separate samples were used for a given well width. The PL linewidths—7.0 meV, 9.6 meV, 11.4 meV (for 50 periods), 15 meV, and 20 meV, for well widths of 120, 75, 50, 30, and 14 Å, respectively—are comparable to the best reported values found in the literature.^{5,10} All PL spectra showed weak satellite peaks due to phonon-assisted recombination. An example, for the 120-Å structure, is shown in Fig. 7. The 1LO line, at $\sim 0.5\%$ of the main peak intensity, is 3–4 times stronger in the quantum wells than in the bulk, with the 2LO line also distinguishable (typically a factor of ~ 30 weaker than the 1LO line). This increased transition strength is, at least in part, likely to be due to the additional localization effect present in quantum wells, namely that due to well-width fluctuations. The assignment of the PL satellites to phonon-assisted transitions is supported by their behavior with temperature. The strength of the 1LO line de-

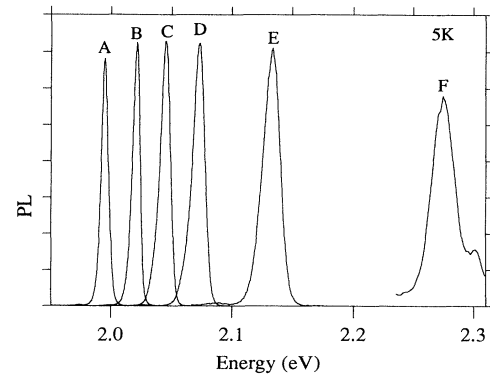


FIG. 6. Composite figure showing 5-K PL of all samples, FWHM linewidth given in brackets. (A) bulk (Ga,In)P, (6.5 meV); (B) 50-period 120-Å MQW (7.0 meV); (C) 50-period 75-Å MQW (9.6 meV); (D) 50-period 50-Å MQW (11.4 meV); (E) 5-period 30-Å MQW (15 meV); and (F) single-period 14-Å quantum well (20 meV).

creases by a factor of ~ 3 over the range 5–40 K. As in the case of bulk material discussed earlier, this can be associated with the thermalization of excitons out of the weakly bound localized states (associated with alloy disorder and/or well-width fluctuations), the resultant decrease in the polarization of the lattice and, thereby, of the exciton-LO-phonon coupling. The energy separation of the main and 1LO peaks decreases roughly by $\sim kT$ over the observed range of 5–70 K, which also supports this assignment because phonon participation allows recombination over the thermal distribution of excitons, unlike the main peak which is constrained to $K \sim 0$ (where K is the exciton center-of-mass wave vector) by momentum conservation.²²

5-K PLE spectra were taken for *all* the quantum-well samples, with the detection energy in each case being on the low-energy edge of the PL line. Examples for the 75 Å and 30-Å well structures are shown in Figs. 8 and 9, respectively. Unlike PL, PLE can closely represent the free-exciton and free-carrier joint density of states and shows the higher-lying, in addition to fundamental, excitonic transitions. Comparison to PL data allows isolation of any Stokes shift due to weak binding in localized

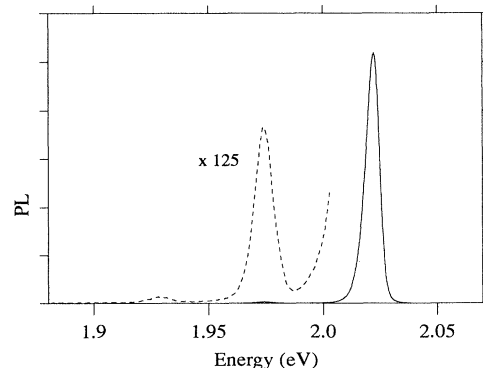


FIG. 7. 5-K PL of the 120-Å MQW showing 1LO and 2LO phonon satellites inset.

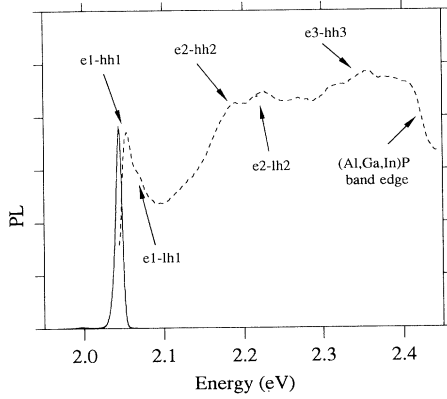


FIG. 8. 5-K PL and PLE for 75-Å MQW. Major transitions are shown in the figure.

states. It is reasonable to expect well-width fluctuations to dominate localization effects for intermediate-width quantum-well samples, and compositional fluctuations in the well and barrier material to dominate for wide and narrow wells, respectively. In the intermediate-width case, the lowest-energy bound-state wave functions are predominantly confined to the well (thus not being strongly affected by barrier compositional fluctuations), but are shifted sufficiently in energy above the bulk absorption edge of the well material by quantum confinement, not to be much affected by compositional fluctuations present in the well itself. This picture is supported by the measured Stokes shifts, which for intermediate well widths are lower than that of the bulk (Ga,In)P. The values are 9.5, 9, 12, 15, and 34 meV, respectively, for the 120-, 75-, 50-, 30-, and 14-Å structures.

The assignments for the main transitions for the 75-Å sample are indicated in Fig. 8. At an energy of ~ 2.4 eV there is a clear falloff in the PL signal which we associate with carriers being created at the band edge of the $(\text{Al}_{0.7}\text{Ga}_{0.3})_{0.52}\text{In}_{0.48}\text{P}$. This band edge appears as a decrease in the PLE signal because e - h pairs that have been created at this particular energy are not reaching the emitting state at which the PLE is being monitored. Figure 9 shows the PL and PLE data obtained from the 30-Å

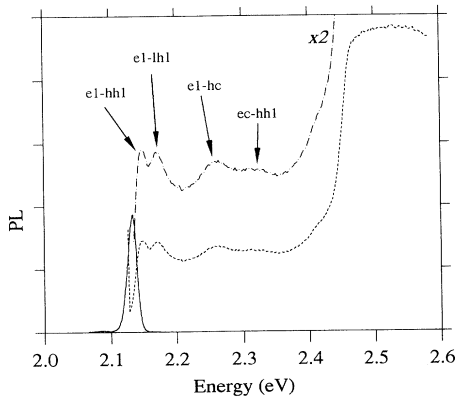


FIG. 9. 5-K PL and PLE for 30-Å MQW. Major transitions are shown in the figure.

well-width sample. Again, the main transition features are identified in the figure. Unlike in the 75-Å case, the (Al,Ga,In)P band edge appears here as an *increase* in the PLE spectrum, indicating an efficient transfer of photo-generated e - h pairs into the (Ga,In)P quantum wells, where they recombine. This difference between the two samples we ascribe to the thicker (Al,Ga,In)P cap layer used in the 75-Å case ($1 \mu\text{m}$ compared to $0.1 \mu\text{m}$ in the 30-Å sample). In the latter PLE spectrum, we can clearly resolve the splitting between the $e1$ -hh1 and $e1$ -lh1 excitonic transitions. Two weaker peaks are evident at 2.258 and 2.318 eV, which we associate with transitions involving one carrier in the continuum while the other is in a confined state. The assignment is $e1$ -hc and ec -hh1, respectively, for the low-energy and high-energy peaks, where hc refers to “above-barrier hole continuum” and ec to “above-barrier electron continuum.”

In order to fit the PLE data, we have made calculations of the expected interband transitions within the envelope-function approximation. In the simple model, all bands are assumed to have a parabolic dispersion. The energy eigenvalues for the electrons and the heavy and light holes are obtained using boundary conditions²³ requiring continuity of the envelope function F and $(1/m^*) (dF/dz)$ at the (Ga,In)P/(Al,Ga,In)P interfaces. Here, z denotes the growth direction of the epitaxial layer. All the necessary input parameters for the model are collected in Table I. E_g is the fundamental energy gap, determined directly from the 5-K PLE data. All other parameters were obtained by linear interpolation between the literature values for the binaries^{24,25} GaP, AlP, and InP. Δ_0 is the spin-orbit splitting, and m_e , m_{hh} , and m_{lh} are, respectively, the electron-, heavy-hole, and light-hole effective masses in the (100) direction. In order to make a comparison between the experimentally measured *exciton* peaks and the calculated intersubband transitions, an adjustment for the exciton binding energy of each transition must be made. Over the range of well widths studied here, it has been calculated²⁶ that the binding energy varies between 11 and 15 meV. For simplicity, we have assumed a constant value of 12 meV for the quantum wells, which introduces only a small error into the calculation which may be neglected.

In Fig. 10 we have plotted the positions of all the transitions (after correction for the exciton binding energy) observed in the PLE spectrum of each sample. The theoretical curves for the $\Delta n = \text{even}$ transitions are also plotted and were generated using a conduction-band discontinuity $\Delta E_c = 0.67\Delta E_g$. We find that this value provides the most comprehensive “fit” to all the observed

TABLE I. Materials parameters used in the envelope-function calculations. Parameters are identified in the text.

Parameter	$\text{Ga}_{0.52}\text{In}_{0.48}\text{P}$	$(\text{Al}_{0.7}\text{Ga}_{0.3})_{0.52}\text{In}_{0.48}\text{P}$
E_g (eV)	2.018	2.456
Δ_0 (eV)	0.096	0.13
m_e/m_0	0.105	0.11
m_{hh}/m_0	0.46	0.51
m_{lh}/m_0	0.14	0.15

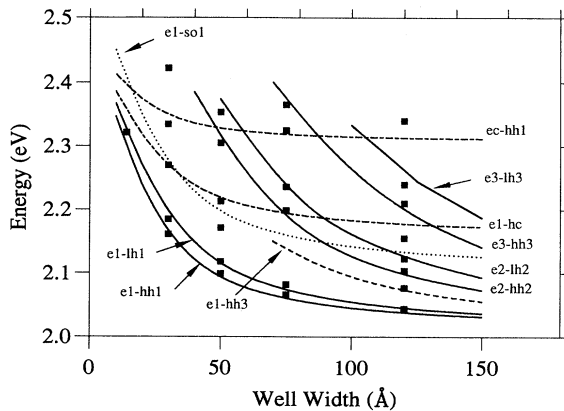


FIG. 10. Transitions measured by PLE for all quantum-well samples (filled squares), with major subbands calculated vs well width using the envelope-function approximation.

transitions. In particular, the light- and heavy-hole splittings are well described by this particular value, as are those features that we have ascribed to transitions involving one confined and one free carrier (i.e., $e1\text{-hc}$ and $ec\text{-hh1}$). We have also calculated the expected value of the $e1\text{-sol}$ transition for this particular system, where sol denotes the first confined level of the spin-orbit split band. In the (Ga,In)P system, the spin-orbit splitting Δ_0 is ~ 100 meV and we assume that the spin split-off hole has an effective mass of $\sim 0.2m_0$, which is a linear interpolation between the values for the binary end members.²⁴ Note that for the 30- and 50-Å samples the $e1\text{-sol}$ and $e1\text{-hc1}$ transitions are almost degenerate, which accounts for the quite large oscillator strength seen at this energy in each case. Finally, we have also plotted the expected transition energies that correspond to the $e1\text{-hc}$ and $ec\text{-hh1}$ transitions. Such transitions were also observed by Liedenbaum *et al.*¹⁰ and are relatively sensitive to the precise size and distribution of the band offsets. With the exception of the cases discussed above when $e1\text{-sol}$ and $ec\text{-hh1}$ are almost degenerate, these transitions involving unconfined MQW states appear as quite weak features in each spectrum. In general, this does not necessarily have to be the case, as the wave functions of the unconfined states can be quite complicated and there is no longer a simple relationship between the number of nodes in the wave function and the energy of the state.^{27,28}

Other measurements of the conduction-band offset given in the literature are $\Delta E_c \sim 0.39$ (Refs. 6 and 9), 0.43

(Ref. 7), 0.6 (Refs. 5 and 8), and 0.65 (Ref. 10). Our results provide strong evidence in support of the latter value, which is the only other measurement to use PLE (with the advantages outlined earlier). Our data are very poorly fit by $\Delta E_c \sim 0.4\Delta E_g$, which has been the generally accepted value,^{6,29} a result in most cases^{6,7} obtained by PL fitting only. In particular, we find that the light-to-heavy-hole splittings are much better reproduced using $\Delta E_c \sim 0.67\Delta E_g$, this being most notable for the 30-Å sample where there is the greatest difference between the two model calculations: the observed splitting is ~ 24 meV, while the calculated value for $\Delta E_c \sim 0.4\Delta E_g$ is 46 meV and for $\Delta E_c \sim 0.67\Delta E_g$ is only 30 meV. Also, higher-energy transitions above 2.3 meV in the 75-Å sample are well described by the transitions $ec\text{-hh1}$ and $e3\text{-hh3}$ if one uses a value of $\Delta E_c \sim 0.67\Delta E_g$, but cannot be described using $\Delta E_c \sim 0.4\Delta E_g$ since there would be no confined $e3$ state with this offset value. Finally, it is worth noting that the deviations between the observed $e1\text{-hh1}$ and $e1\text{-lh1}$ transitions and those of the calculation assuming $\Delta E_c \sim 0.67\Delta E_g$, can easily be accommodated by a slight adjustment (a few percent) of the nominal well widths.

IV. SUMMARY

5-K photoluminescence and photoluminescence excitation spectra have been measured for $\text{Ga}_{0.52}\text{In}_{0.48}\text{P}/(\text{Al}_{0.7}\text{Ga}_{0.3})_{0.52}\text{In}_{0.48}\text{P}$ bulk and quantum-well epilayers, grown under conditions in which the data are not influenced by alloy ordering effects. The band-gap and excitonic binding energy have been determined to be 2.018 and ~ 8.1 meV, respectively, for bulk $\text{Ga}_{0.52}\text{In}_{0.48}\text{P}$. Comparison between the PL and PLE measurements has allowed the isolation of energy shifts due to weak excitonic localization. A conduction-band discontinuity of $\Delta E_c \sim 0.67\Delta E_g$ has been determined to provide the best fit to all transitions observed in PLE for quantum wells of width ranging from 14 to 120 Å.

ACKNOWLEDGMENTS

The authors thank A. Staton-Bevan, X. Zhang, and B. A. Joyce (Imperial College, London, U. K.) for the TEM and TED measurements; Epitaxial Products International, Cardiff, U. K.; and R. P. Bryan and G. R. Olbright of Photonics Research, Inc. for helpful discussions and making available a copy of their unpublished manuscript.

¹H. C. Casey and M. B. Panish, *Heterostructure Lasers, Part B: Materials and Operating Characteristics* (Academic, New York, 1978), Chap. 5.

²A. Valster, J. v. d. Heijden, M. Boermans, and M. Finke, *Philips J. Res.* **45**, 267 (1990).

³A. Gomyo, T. Suzuki, and S. Iijima, *Phys. Rev. Lett.* **60**, 2645 (1988).

⁴S.-H. Wei and A. Zunger, *Phys. Rev. B* **39**, 3279 (1989).

⁵R. P. Schneider, R. P. Bryan, J. A. Lott, E. D. Jones, and G. R. Olbright, *J. Cryst. Growth* **124**, 7633 (1992).

⁶T. Hayakawa, K. Takahashi, M. Hosoda, S. Yamamoto, and T. Hijikata, *Jpn. J. Appl. Phys.* **27**, 1553 (1988).

⁷H. Tanaka, Y. Kawamura, S. Nojima, K. Wakita, and H. Asahi, *J. Appl. Phys.* **61**, 1713 (1987).

⁸M. Ikeda, K. Nakano, Y. Mori, K. Kaneko, and N. Watanabe, *J. Cryst. Growth* **77**, 380 (1986).

⁹M. O. Watanabe and Y. Ohba, *Appl. Phys. Lett.* **50**, 906 (1987).

¹⁰C. T. H. F. Liedenbaum, A. Valster, A. L. G. J. Severens, and G. W. t'Hooft, *Appl. Phys. Lett.* **57**, 2699 (1990).

¹¹M. D. Scott and P. Rees (private communication).

- ¹²R. Osorio, J. E. Bernard, S. Froyen, and A. Zunger, *Phys. Rev. B* **45**, 11 173 (1992).
- ¹³T. Suzuki, A. Gomyo, S. Iijima, K. Kobayashi, S. Kawata, I. Hino, and T. Yuasa, *Jpn. J. Appl. Phys.* **27**, 2098 (1988).
- ¹⁴J. E. Fouquet, V. M. Robbins, J. Rosner, and O. Blum, *Appl. Phys. Lett.* **57**, 1566 (1990).
- ¹⁵H. Hamada, M. Shono, S. Honda, R. Hiroshima, K. Yodoshi, and T. Yamaguchi, *IEEE J. Quantum Electron.* **27**, 1483 (1991).
- ¹⁶A. Gomyo, T. Suzuki, S. Iijima, H. Hotta, H. Fujii, S. Kawata, K. Kobayashi, Y. Ueno, and I. Hino, *Jpn. J. Appl. Phys.* **27**, L2370 (1988).
- ¹⁷X. Zhang, A. Staton-Bevan, and B. A. Joyce (private communication).
- ¹⁸A. Mascarenhas, S. Kurtz, A. Kibler, and J. M. Olson, *Phys. Rev. Lett.* **63**, 2108 (1989).
- ¹⁹M. Kubo, M. Mannoh, and T. Narusawa, *J. Appl. Phys.* **66**, 3767 (1989).
- ²⁰T. A. Gant, M. Dutta, N. A. El-Masry, S. M. Bedair, and M. Stroschio, *Phys. Rev. B* **46**, 3834 (1992).
- ²¹K. J. Nash and M. S. Skolnick, *Phys. Rev. B* **39**, 5558 (1989).
- ²²H. B. Bebb and E. W. Williams, in *Semiconductors and Semimetals*, edited by R. K. Willardson and A. C. Beer (Academic, New York, 1972), Vol. 8, pp. 293–295.
- ²³D. J. Ben Daniel and C. B. Duke, *Phys. Rev.* **152**, 683 (1966).
- ²⁴*Numerical Data and Functional Relationships in Science and Technology*, edited by O. Madelung, Landolt-Börnstein, New Series, Group III, Vol. 17, Pt. a (Springer-Verlag, New York, 1982).
- ²⁵*GaInAsP Alloy Semiconductors*, edited by T. P. Pearsall (Wiley, New York, 1982), Appendix.
- ²⁶G. Duggan (unpublished).
- ²⁷J. J. Song, Y. S. Yoon, A. Fedotowsky, Y. B. Kim, J. N. Schulman, C. W. Tu, D. Huang, and H. Morkoç, *Phys. Rev. B* **34**, 8958 (1986).
- ²⁸S. H. Pan, H. Shen, Z. Hang, F. H. Pollak, W. Zhuang, Q. Xu, A. P. Roth, R. A. Masut, C. Lacelle, and D. Morris, *Phys. Rev. B* **38**, 3375 (1988).
- ²⁹G. Hatakoshi, K. Itaya, M. Ishikawa, M. Okajima, and Y. Uematsu, *IEEE J. Quantum Electron.* **27**, 1476 (1991).